

Modeling and simulation of wetting and spreading phenomena for thin liquid films

Leonard W. Schwartz¹

(Received 31 July 2007; revised 01 October 2007)

Abstract

We present a mathematical model for the slow three-dimensional motion of a liquid coating on a substrate with wetting and de-wetting edges. The equilibrium contact angle is considered to be a material property of the liquid-substrate system. Substrate chemical heterogeneity, or physical roughness, may also be an important determinant of edge motion. Conversely, dynamic contact angle information is not required by the model; it is predicted as part of the solution. Calculated results are compared with experimental observation with good agreement. Many industrial applications involve liquid coating and wetting considerations are usually quite important.

Contents

1 Introduction

C70

See <http://anziamj.austms.org.au/ojs/index.php/ANZIAMJ/article/view/348> for this article, © Austral. Mathematical Soc. 2007. Published October 10, 2007. ISSN 1446-8735

1	<i>Introduction</i>	C70
2	Outline of the model	C71
3	Some applications of the model	C75
4	About dynamic contact angles	C78
	References	C81

1 Introduction

It has been known for some time that the governing equations for viscous fluid flow can be considerably simplified if the flow boundaries and the streamlines are almost parallel. The theory has been used with great success to describe flow in fully flooded regions between rigid moving boundaries, as in oil filled bearings where the lubricant is used to prevent metal-to-metal contact [18]. The approximation is commonly known as *lubrication theory* and can also be used to good effect when one of the liquid boundaries is free, as is the case for a thin liquid coating or paint layer [1, 2]. For these thin layer flows, particular attention is required to allow the advancement or recession of contact lines, the three phase intersection where liquid, solid and vapor meet. It is now well known that the usual no-slip boundary condition, applied where a liquid meets a solid, must be weakened near moving contact lines [9].

Here we give an outline of the mathematical model, including a simple coupled equation model, that is meant to emulate the effects of evaporation and drying. We then show the type of results that can be calculated using this model and show how they compare with experiment. Finally we discuss the important question of dynamic contact angles, and the possible existence of contact line angle and speed relationships. We point out how our model differs from some others.

2 Outline of the model

The lubrication approximation is invoked to find an unsteady evolution equation for a number of coating flow problems. Provided that the inclination of liquid boundaries, Reynolds number $\rho U h / \mu$, and capillary number $\mu U / \sigma$ are all sufficiently small, quantitative accuracy can be maintained. The statement of mass conservation is

$$h_t = -\nabla \cdot \mathbf{Q} - V, \quad (1)$$

where the areal flux vector \mathbf{Q} arises from several different effects. A representative equation, including some but not all of the effects that can be considered, is [1, 2, 6, 14]

$$h_t = -\nabla \cdot \frac{\sigma h^3}{3\mu} \left(\nabla \nabla^2 h - \frac{\rho g}{\sigma} \nabla h + (1/\sigma) \nabla \Pi \right) - \frac{h^2}{2\mu} \nabla \cdot \tau - \frac{\rho \omega^2}{3\mu} \nabla \cdot (r h^3 \mathbf{e}_r) - V. \quad (2)$$

Here h is the liquid film thickness, μ is viscosity, t is time, and ∇ is a two dimensional operator in the substrate coordinates. The terms on the right represent the effects of surface tension σ , gravity, ‘disjoining pressure’ Π , shear stress τ , and centrifugal force. Not all terms need be present in any given problem, and there are sometimes other effects that require inclusion. Π may take on a number of functional forms. However the associated local energy density e , satisfying $de/dh = -\Pi$, should have a local minimum for $h = h^*$, where h^* is a ‘slip thickness’ that is required because of the impossibility of moving a contact line without violating the no-slip condition [9, 11]. One choice is

$$\Pi = B \left[\left(\frac{h^*}{h} \right)^n - \left(\frac{h^*}{h} \right)^m \right], \quad n > m > 1,$$

where B prescribes θ_e , the equilibrium contact angle. In fact θ_e is a physical property of the three phase solid, liquid, gas system. It can vary from point to point on the substrate; thus $\theta_e = \theta_e(x, y)$ for a heterogeneous substrate.

The concept of disjoining pressure and how it determines θ_e was formulated by Frumkin [7] and Deryaguin [5].

The last term on the right side of equation (1) or (2) is V , the evaporation rate, with the dimensions of speed. Often the evaporation rate is an additional unknown and needs to be calculated in terms of the local mixture composition, as discussed below.

Irrespective of the choice of driving terms, for ‘slow’ flows where kinetic energy is negligible, the evolution equation (1) or (2) is equivalent to an energy equation of the form

$$\dot{E}_\mu = -\frac{d}{dt} E_{\text{stored}}. \quad (3)$$

Here \dot{E}_μ is the instantaneous rate of viscous energy dissipation. E_{stored} is the total system energy and includes integrated interfacial and other potential energy components, corresponding to terms on the right side of (1) or (2). There is also a principle that, in slow motion, the system will take the ‘path of least resistance,’ subject to problem specific constraints. This is the cause of a variety of ‘pattern forming instabilities.’ Figures 1–4 show frames from simulations that illustrate the nonlinear evolution caused by instability. The examples are relevant to industrial applications. We choose to use these examples because experimental pictures are also available.

A ubiquitous phenomenon for liquid coatings is drying. Whereas the physics and chemistry of drying are complicated, and incompletely understood, progress can be made by constructing a simplified model. For example, certain binary liquid mixtures have surface tension values that vary with the fractional composition. A commonplace example is an alkyd paint whose surface tension increases as the solvent evaporates. Strong surface tension gradient effects can arise for a thin, nonuniform coating layer of the mixture. The gradient of surface tension $\nabla\sigma$ is equivalent to an applied shear stress τ on the liquid free surface [10], as in equation (1) or (2). Often, there is surprising behavior; an initial hump in the coating may turn into a local

depression in the final dry coating.

The model can be extended to reproduce phenomena associated with drying. A conservation equation for the non-evaporating ‘resin’ fraction c is [14]

$$\frac{\partial(ch)}{\partial t} = \nabla \cdot (Dh\nabla c - c\mathbf{Q}) . \quad (4)$$

The two partial differential equations (1) or (2) and (4) are solved simultaneously for the layer thickness h and the resin fraction c . Additional relations must be supplied that relate the viscosity μ , the diffusivity D , the surface tension σ and the evaporation rate V of the solvent fraction. This simple drying model postulates a known relation between evaporation rate and local mixture composition. Admittedly, this is an oversimplification of the relevant thermodynamics.

Invariably, the thickness of a liquid film or coating is much smaller than characteristic lengths in the filmwise direction. Thus an important simplification that has been exploited above is to assume that the coating properties are constant across the thin dimension. This is plausible because the coating layer is very thin and diffusional mixing of the mixture components across this small distance can be expected to happen more rapidly than changes along the film. This well mixed assumption has previously been used in two dimensional flow models by us and others [14]. Not all coating mixtures are adequately handled by this model. Coatings that develop a significant skin above a fluid underlayer as they dry require use of a more complicated model than that presented here.

Equations (1) or (2) and (4) are solved simultaneously by finite difference methods. Typically, we solve the system on a rectangular grid; the moving contact lines are ‘captured’ rather than ‘tracked.’ That is, the evolution equations are solved over the entire computational domain including the nominally dry areas. Contact lines appear where finite thickness regions meet the $h \approx h^*$ slip layer. Alternating direction implicit methods work well for these ‘heat like’ problems [12].

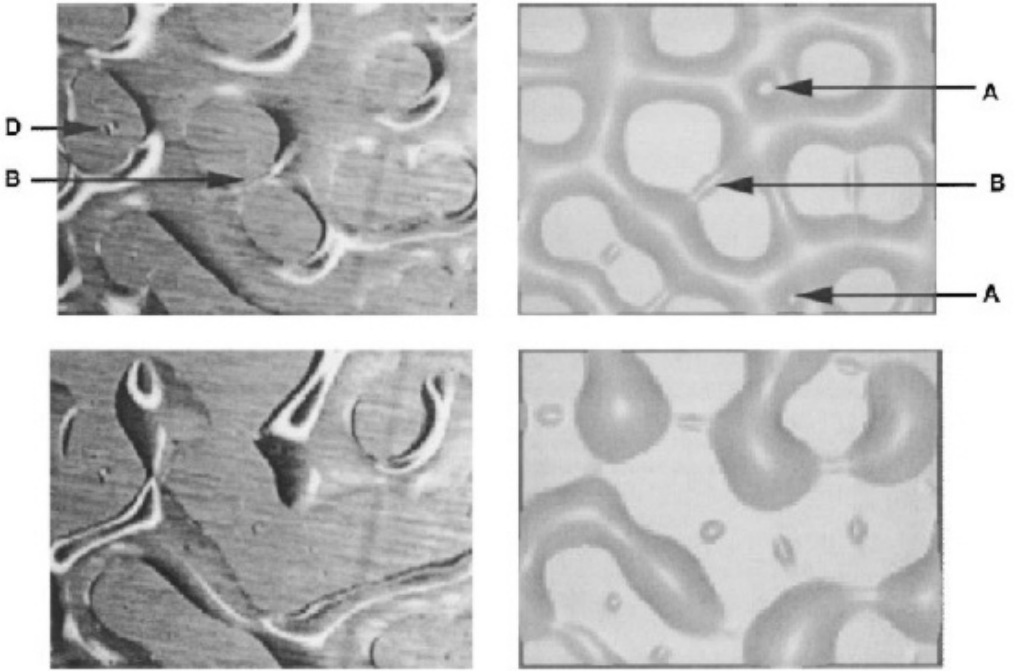


FIGURE 1: Breakup and evaporation of an originally continuous, liquid film on a waxy substrate. Experimental micrographs and frames from a simulation are shown at two times. The detailed patterning is caused by a few easily observed substrate defects, such as label ‘D’ in the micrograph. Label ‘B’ in both the micrograph and the simulation shows a thin filament that is about to break. Filament breakage leaves small residual drops, as seen in the lower pictures. The pattern has become almost immobile due to drying in the lower pictures.

3 Some applications of the model

Figure 1 shows the breakup of an originally continuous liquid film, similar to the ‘balling up’ of a water film on a waxed car. Experimental micrographs and simulation are shown [14]. The coating de-wets on a heated plate and leaves behind a waxy residue. Here the relevant physics includes evaporation and finite contact angle effects using a given spatially dependent variation in the prefactor B in the expression for the disjoining pressure Π . The coupled system (1) or (2) and (4) is used in the simulation. Note the strong qualitative agreement between simulation and observation. Although dewetting patterns often seem to be random, in this experiment the detailed patterning is caused by a few easily observed substrate defects. The locations of the observed defects were used as nucleation sites or ‘seeds’ to start the simulation. The seed locations were modeled as spots of larger contact angle θ_e . The initial rate of dewetting is proportional to the value of B on the defects. In order to match the time scale in the experiment, the B value on the defects was taken to be 15 percent larger than the value on the surrounding field. All other physical input parameters in the mathematical model used experimentally measured values.

Subsequent breakup is largely deterministic and significant similarity between observation and prediction is seen. Isolated small droplets, resulting from the snapping of thin liquid filaments, are larger in the simulation than in the experiment. This is a coarse grid effect and would be lessened if the calculation had used a finer mesh.

Figure 2 gives a comparison of simulation results for spin coating (left) with experimental pictures (right). Spin coating is used in the electronics industry to produce very uniform thin films. Both simulation and experiment show the development of the characteristic ‘wall and tower’ structure [15]. The center of rotation is near the lower right corner for each picture. The interval between frames is about 0.1 second. Only one-quarter of an assumed four-fold symmetric pattern is calculated in the simulation. The experiment

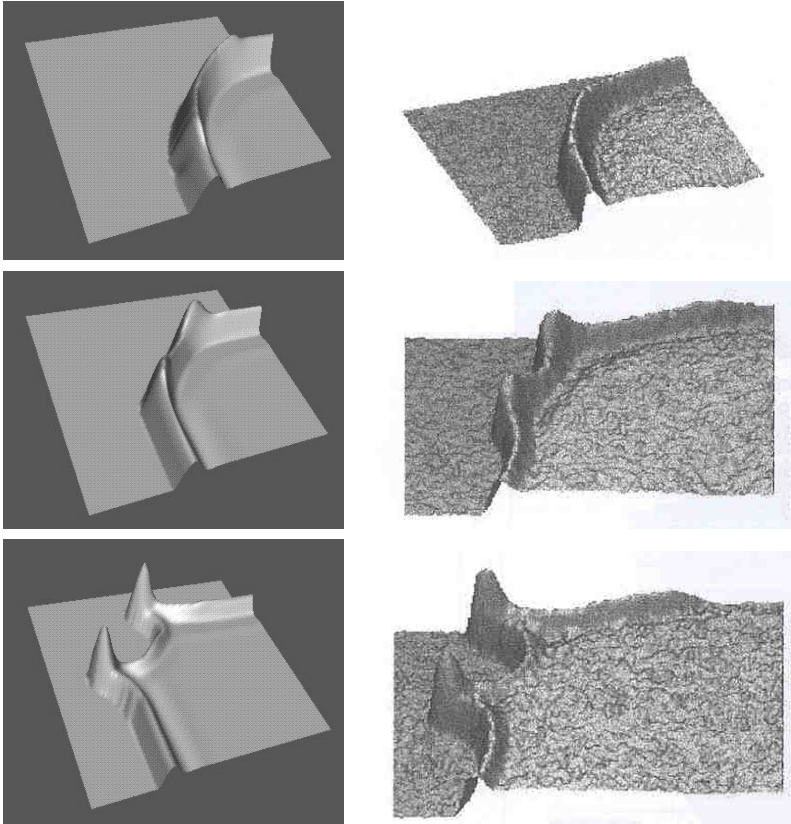


FIGURE 2: A comparison of simulation results for spincoating (left) with experiment (right). Both show the development of the characteristic ‘wall and tower’ structure. The center of rotation is near the lower right corner for each picture. The interval between frames is about 0.1 second. Only one-quarter of an assumed four-fold symmetric pattern is calculated in the simulation.

was performed by Dr Jeroen Lammers and colleagues of the Philips Research Laboratory in The Netherlands [8]. The calculation was performed in a rotating coordinate system while the experiment used the equivalent of a strobe light to remove the rotational component of frontal motion. Experimentally, the coating thickness field was measured by light absorption. The ‘towers’ have been driven outward by centrifugal force, resulting in a pattern of ‘fingers.’ Since complete wetting of the substrate is usually required in applications, such fingering needs to be avoided. The simulation used a contact angle value of 4.7 degrees while the experimentally measured value was ‘about 4 degrees.’ Drying effects are ignored since the spin process is relatively rapid.

Surface tension is usually a decreasing function of temperature; thus a thermal gradient on a substrate will produce a surface tension gradient that is equivalent, approximately, to an applied surface shear stress. Experiments have been performed on a vertical metal plate that is partially submerged in a liquid bath. By cooling the top end of the plate, the resulting shear stress causes a thin film of liquid to climb up the plate. The moving front of the rising film is unstable and results in fingers as shown in Figure 3. The interferometric pictures are from Cazabat et al. [4]. The model calculations are from Eres et al. [6].

Figure 4 shows the fate of a draining drop on a window pane. Note the complicated breakup pattern [15]. It may be compared with an experimental picture on the far right [13]. Interestingly, these apparently complicated patterns are really highly structured. Starting from rest, as a static sessile drop at the equilibrium contact angle θ_e , the calculated pattern exhibits several different length scales. Only gravity, surface tension, and constant θ_e disjoining pressure are used in the simulation. The simplified theory yields a single control parameter

$$G_p = \frac{2\rho g}{\sigma} \left(\frac{4V}{\pi} \right)^{2/3} \frac{1}{\theta_e^{5/3}}, \quad (5)$$

where V is the drop volume [16]. Thus, within this theory, all rain drops of

a given volume must have an identical history, as in the figure. Since θ_e is constant, this history is only correct for an ideally clean window pane. A dirty window pane can be modeled using spots of contamination. This is easily introduced into the simulation and will give other patterns, of course.

4 About dynamic contact angles

We believe it is remarkable that such a relatively simple theory can predict a wide variety of complicated results. Thus, according to ‘Occam’s Razor’,¹ this model should be preferred. Conversely, some workers introduce an additional equation, ab initio [3, 17]; the algorithm is of the form

$$U = f(\theta_d; \theta_e), \quad (6)$$

where U is the local normal speed at the wetting line and θ_d is the dynamic contact angle. While it is usually true that $\theta_d > \theta_e$ when $U > 0$ and $\theta_d < \theta_e$ when $U < 0$, no such local relationship should be a postulate of a physical model of wetting, for a variety of reasons:

1. Consider two *forced* spreading processes: spin coating driven by centrifugal force and metered gravitational flow of a uniform coating layer onto an inclined wall. In either case, the speed of frontal advance is essentially determined by forces that are remote from the moving front, for example drop volume and spin speed in the first case, and volumetric flow rate and gravity in the second. Equation (6) can be made dimensionally correct only by specifying length and time scales. These scales will depend on the remote driving mechanisms which are quite different in the two cases.

¹Mediaeval philosopher William of Occam stated that ‘one should not increase, beyond what is necessary, the number of entities required to explain anything.’

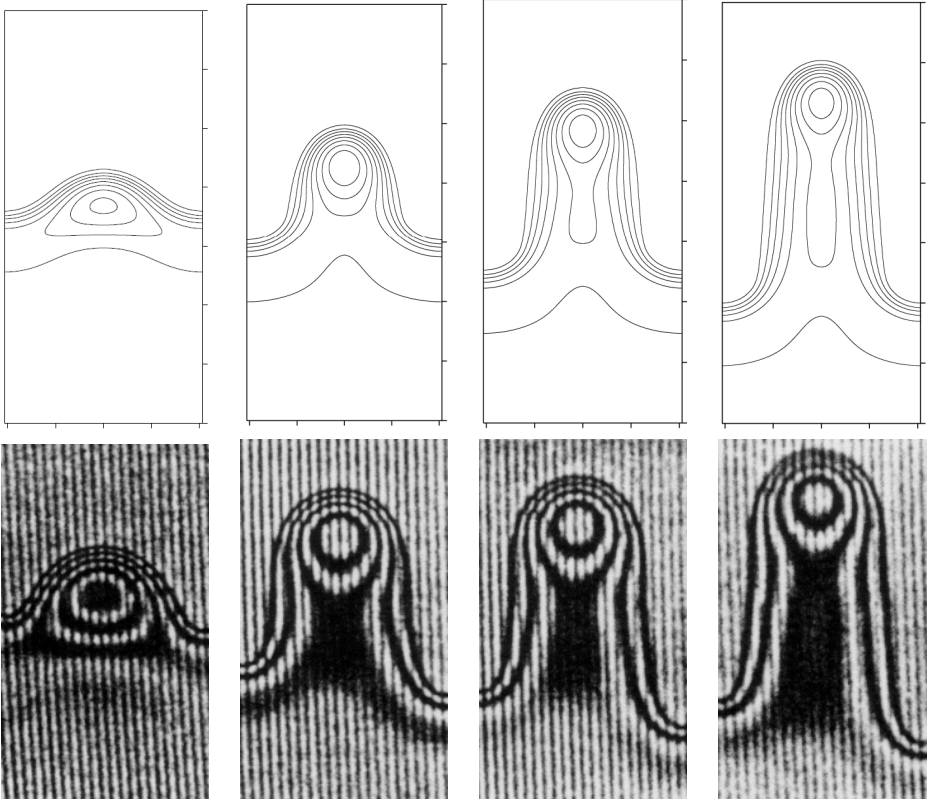


FIGURE 3: Thermal gradient causes fingering rise on a vertical metal plate in a liquid bath. Simulation results are shown on top at four times and the corresponding interferometric pictures are on the bottom.

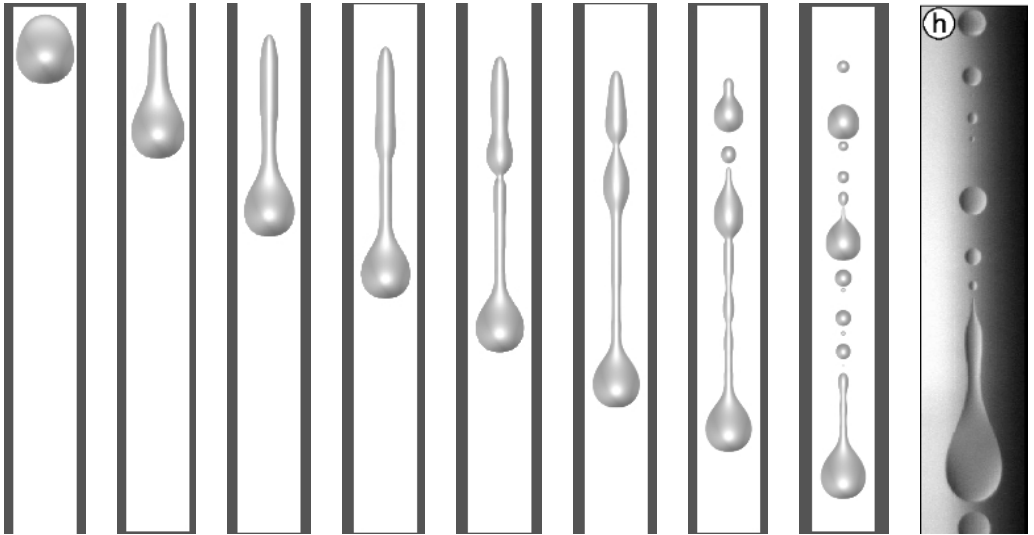


FIGURE 4: A draining drop on a window pane showing the complicated breakup pattern. Eight frames from a simulation are shown at eight different times. An experimental picture is on the far right for comparison. Note that, for the simulation pictures, the frames have been transposed upward as time proceeds.

2. The equations of fluid mechanics that govern the slow motion of coating liquids are *elliptic* in character. Thus the dynamic angle at any point will be influenced by motions, boundaries, etcetera that are remote from that point.
3. Even the static contact angle requires careful definition. The equilibrium contact angle θ_e must be determined from, say, a sessile axisymmetric droplet on a uniform horizontal substrate. Equation (6) implies that the static angle must be unique if the droplet is not moving. This is not true for a droplet that is held stationary on a dirty or cracked window. The minimum energy configuration will thus have many contact angle values on the same substrate.

References

- [1] Atherton, R. W. and Homsy, G. M., On the derivation of evolution equations for interfacial waves, *Chem. Eng. Comm.* **2**, 57, 1976. C70, C71
- [2] Benney, D. J., Long waves on liquid films, *J. Math. and Phys.* **45**, 150, 1966. C70, C71
- [3] Blake, T. D., “Dynamic contact angles and wetting kinetics.” In: J. C. Berg (ed.) *Wettability*, Marcel Dekker, New York, 251–309, 1993. C78
- [4] Cazabat, A. M., Heslot, F., Carles, P. and Troian, S. M., Hydrodynamic fingering instability of driven wetting films, *Adv. Colloid Interf. Sci.* **39**, 61–75, 1992. C77
- [5] Deryaguin, B. V., Theory of the capillary condensation and other capillary phenomena taking into account the disjoining effect of long-chain molecular liquid films, *Zhur. Fiz. Khim.* **14**, 137 (1940) [In Russian]. C72

- [6] Eres, M. H., Schwartz, L. W., and Roy, R. V., Fingering phenomena for driven coating films, *Physics of Fluids* **12**, 1278–1295, 2000. [C71](#), [C77](#)
- [7] Frumkin, A. N., On the phenomena of wetting and sticking of bubbles, *Zhur. Fiz. Khim.* **12**, 337 (1938) [In Russian]. [C72](#)
- [8] Haze, R. and Lammers, J. H., “Liquid height measurement through light absorption,” Philips Research Laboratory, Report No. UR 819/99, Eindhoven, Netherlands, 1999. [C77](#)
- [9] Huh, C. and Scriven, L. E., Hydrodynamic model of steady movement of a solid/liquid/fluid contact line, *J. Colloid Interface Sci.* **35**, 85, 1971 . [C70](#), [C71](#)
- [10] Levich, V. G., *Physicochemical Hydrodynamics*, 1962, Prentice–Hall, Englewood Cliffs. [C72](#)
- [11] Moriarty, J. A. and Schwartz, L. W., Effective slip in numerical calculations of moving-contact-line problems, *J. Engineering Math.* **26** 81–86, 1992. [C71](#)
- [12] Peaceman, D. W. and Rachford, H. H., The numerical solution of parabolic and elliptic differential equations, *SIAM J.* **3**, 28, 1955. [C73](#)
- [13] Podgorski, T., Flesselles, J.-M., and Limat, L., Corners, cusps, and pearls in running drops, *Phys. Rev. Lett.* **87**, 1–4, 2001. [C77](#)
- [14] Schwartz, L. W., Roy, R. V., Eley, R. R. and Petrash, S. Dewetting Patterns in a Drying Liquid Film, *J. Colloid Interface Science* **234**, 363–374, 2001. [C71](#), [C73](#), [C75](#)
- [15] Schwartz, L. W. and Roy, R. V., Theoretical and numerical results for spin coating of viscous liquids, *Physics of Fluids* **16**, 569–584, 2004. [C75](#), [C77](#)

- [16] Schwartz, L. W., Roux, D. and Cooper-White, J. J., On the shapes of droplets that are sliding on a vertical wall, *Physica D* **209**, 236–244, 2005. [C77](#)
- [17] Seeberg, J. E. and Berg, J. C.. Dynamic wetting in the low capillary number regime. *Chem. Eng. Sci.* **47** 4455–4464, 1992. [C78](#)
- [18] Sherman, F. S., *Viscous Flow*, 1990, McGraw–Hill, New York. [C70](#)

Author address

1. **Leonard W. Schwartz**, Department of Mechanical Engineering, University of Delaware, Newark, DE 19716, USA.
<mailto:schwartz@udel.edu>